

CHARACTERISTICS OF SUBCRITICAL FLOW OVER VERTICAL DROPS WITH SLOPING APRONS*

M. R. CHAMANI^{1**}, M. K. BEIRAMI¹, N. RAJARATNAM² AND A. A. DEGHANI³

¹Dept. of Civil Engineering, Isfahan University of Technology (IUT), Isfahan, I. R. of Iran, 84156-83111
Email: mchamani@cc.iut.ac.ir

²Professor Emeritus, University of Alberta, Edmonton, Alberta, Canada T6G 2W2

³Dept. of Water Engineering, Gorgan University of Agricultural Sciences & Natural Resources, Gorgan, I. R. of Iran

Abstract– In this investigation, characteristics of vertical drops with subcritical flow at the upstream channel and sloping aprons at the downstream channel have been studied experimentally. Flow characteristics such as pool depth, downstream depth, and energy loss have been measured. Two physical models of 0.41 and 0.21 m height were built and the inverse slope was set at 5°, 10° and 15° degrees. Experimental data were compared with the previous investigators' results for horizontal downstream channels. A method is presented to estimate flow characteristics. It was shown that the values of the relative pool depth for sloping aprons are larger than those with a horizontal downstream channel. It was found that the values of the relative downstream depth for sloping aprons are slightly larger than those with a horizontal downstream channel. Experimental results show that the relative energy loss increases by increasing the angle of the invert and the maximum increase is for the 5° degree slope. Predictions for the pool and downstream depths agree with the experimental data, but the differences between the predictions and the experimental results of the relative energy loss are significant.

Keywords– Hydraulic structures, subcritical flow, drop, sloping apron

1. INTRODUCTION

In irrigation channels, drops are necessitated where the topography is steeply sloping. To reduce earth fill expenses in locations where channel slopes are less than the ground slopes, drops are provided. A vertical drop is a structure where the flow passes over a vertical fall and descends into the stilling pool, downstream of the drop. Drops are generally categorized to be inclined or vertical. Vertical drops are also divided into four types according to their geometrical shapes, as shown in Fig. 1. Energy loss is achieved through turbulent mixing in the pool created downstream of the drop. The flow upstream a drop can be either subcritical or supercritical. For subcritical flow, the flow passes through critical depth in the channel just upstream of the drop and then overflows the drop brink. For supercritical flow, the upstream depth is less than the critical depth and is a function of the Froude number and discharge.

Investigations on the hydraulic characteristics of vertical drops with subcritical flow and horizontal apron in the downstream channel were made [1-6]. In White's discussion [3], a theoretical solution for energy loss was presented based on the impinging jet simulation, which was later corrected by Gill [4]. Rand [5] presented empirical equations in terms of a dimensionless parameter for the evaluation of flow characteristics. Rajaratnam & Chamani [6] examined the assumptions made by White and Gill and developed a new method to predict the energy loss.

*Received by the editors April 14, 2007; Accepted January 20, 2008.

**Corresponding author

This paper presents the results of an experimental study on vertical drops with subcritical flow in the upstream channel and an adverse slope in the downstream channel (Fig. 1c). A method has been presented to evaluate flow characteristics such as the pool depth, downstream depth and energy loss at the drop.

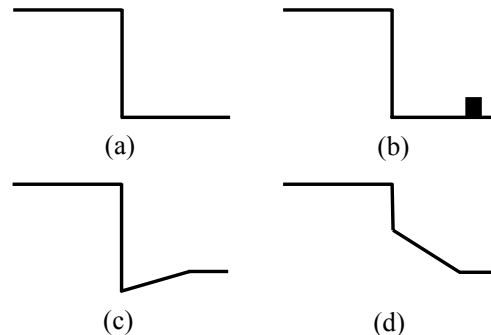


Fig. 1. Types of vertical drops; a) Vertical drop with horizontal slope in the downstream channel, b) Baffle vertical drop, c) Vertical drop with adverse slope in downstream channel, d) Vertical drop with positive slope in downstream channel

2. EXPERIMENTAL ARRANGEMENTS AND RESULTS

The experimental setup is similar to that shown in [7]. A 0.405 m wide, 11 m long channel with variable heights (0.7 m to 1.2 m) was used. Two ventilated vertical drops with heights of $h = 0.21$ m and 0.41 m were placed in the channel. A length of $\ell = 0.65$ m of the channel bed immediately downstream of the drop was inclined (Fig. 2). In Fig. 2, d_c is the critical depth, d_f the pool depth, θ the angle of the apron, L_d the drop length, and d_l the flow depth at downstream. For $h = 0.21$ m, the angle of the inclined apron was set at $\theta = 5^\circ$, while for $h = 0.41$ m, the angles were $\theta = 5^\circ, 10^\circ$ and 15° degrees. For $\theta > 15^\circ$, the effective height of the drop (difference between the bed levels at the upstream and downstream channels) would be small and because of the rise of the pool depth, ventilation of the drop would be difficult. In addition, the relative discharge ratio (d_c/h' where $h' = h - \ell \sin\theta$, is the effective drop height) becomes too large and is not recommended for practical purposes.

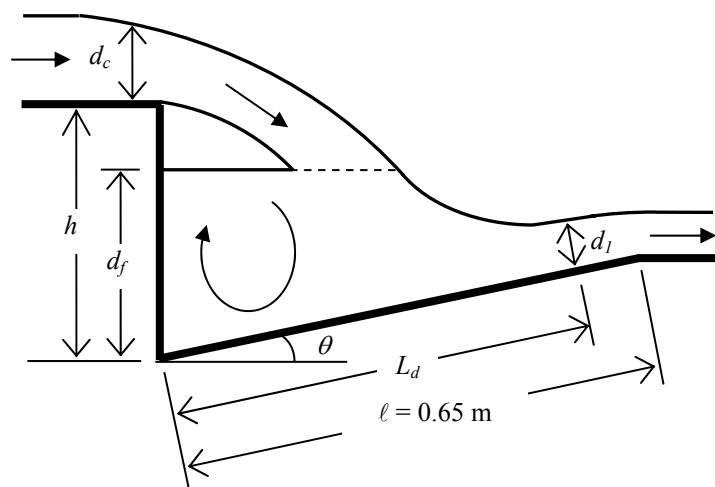


Fig. 2. Definition sketch of a drop

Water flowed to the drop from the laboratory reservoir through the stilling tank above the flume. The discharge was measured by means of a turbine flow meter installed in the supply line. The subcritical flow

was created by extending the drop into the stilling tank. Two flow regimes have been observed. For small discharges, the flow remains subcritical downstream of the drop. By increasing the discharge, the second regime occurs where the flow is supercritical downstream of the drop. In this investigation, the second regime has been studied.

Table 1 shows the results of the experiments on two drops with heights of 0.21 m (model I) and 0.41 m (model II). A total of 18 tests was run for the two drops, providing a range of discharge from 7 l/s to 60 l/s and d_c/h' from 0.12 to 0.54.

Table 1. Experimental data

h (m)	θ	h' (m)	Q (l/s)	d_c/h'	d_1/h'
0.21	5°	0.153	10.6	0.57	0.14
			12.4	0.64	0.14
			17.8	0.75	0.18
			23.2	0.84	0.22
			30.4	0.96	0.27
0.41	5°	0.353	11.6	0.30	0.04
			21.0	0.42	0.07
			31.9	0.54	0.10
			44.9	0.65	0.13
			56.9	0.72	0.17
0.41	10°	0.297	13.0	0.50	0.07
			23.7	0.64	0.10
			36.3	0.78	0.13
			49.9	0.91	0.17
0.41	15°	0.242	23.2	0.90	0.14
			27.4	1.00	0.16
			36.2	1.10	0.20
			44.3	1.18	0.22

It is found that the boundaries between the two regimes exhibit hysteresis effects. For a specific drop height, the discharge at which the subcritical regime changes to the supercritical regime is different when the discharge is increased or decreased. For example, for a drop with $h = 0.21$ m and $\theta = 5^\circ$, the discharge at which the flow changes from subcritical regime to supercritical regime is 5.7 l/s, while for decreasing the discharge, the discharge limit is 10.1 l/s. This is similar to Wu and Rajaratnam where the effect of tailwater on flow regimes at rectangular sharp crested weirs and drops are studied [8-9]. In these studies, a parameter $\lambda_a = \left[\frac{\sqrt{g(d_c - y_u)}}{(q/y_t)} \right]$ is used to characterize the limits at which different flow regimes occur, where y_u is the depth of tailwater above the upstream channel bed, q the discharge per unit length, and y_t the tailwater depth above the downstream channel bed.

Additional experiments were performed to find the boundaries between the two regimes. For each drop height, the discharge was varied to find the discharge at which the flow regime changes. Experiments were performed with both increasing and decreasing discharges, with the changes being made very gradually. By defining $\lambda_b = \left[\frac{\sqrt{g(h' - d_c)}}{(q/d_1)} \right]$, the variation of the relative discharge against λ_b is presented in Fig. 3. In Fig. 3, zones I and III are the regions where supercritical flow and subcritical flows occur, respectively. Zone II is a transition zone where either supercritical or subcritical regimes can occur depending on the discharge falling or rising. The following mean curves are presented for the limits of the flow regimes.

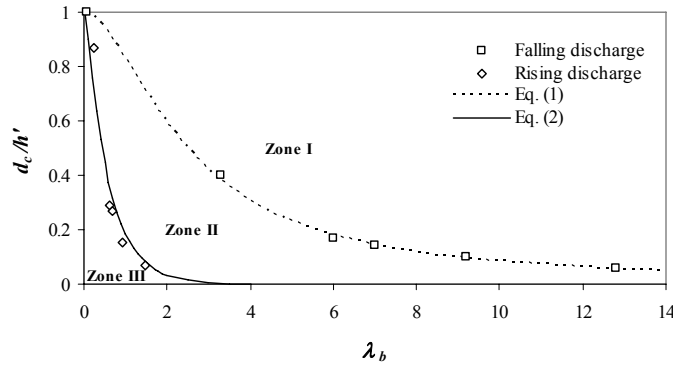


Fig. 3. Limits for supercritical and subcritical flow regimes at drops

$$\frac{d_c}{h'} = \frac{1}{1 + 0.206\lambda_b^{1.726}} \quad \text{falling discharge } (R^2 = 0.999) \quad (1)$$

$$\frac{d_c}{h'} = 1.0734e^{-1.751\lambda_b} \quad \text{rising discharge } (R^2 = 0.978) \quad (2)$$

3. PREDICTION METHOD FOR FLOW FEATURES AT THE DROP

This method is based on the extension of models by White, Rand and Gill, presented for drops with horizontal aprons [3-5]. Consider a drop located in a rectangular channel as shown in Fig. 4. The flow approaching the drop is subcritical and the flow immediately downstream of the drop is supercritical. The following hypotheses may be retained: effects of air entrainment and bed shear stresses are neglected and the pressure distribution along the drop wall is assumed to be hydrostatic. The later assumption is not justified by any experimental works, but it is used by [2, 3, 4, 6] to develop relevant theories. Applying the momentum equation in the horizontal direction to the control volume I (CVI), we obtain (Fig. 4)

$$\frac{1}{2}\gamma d_c^2 + \frac{1}{2}\gamma d_f^2 - \frac{1}{2}\gamma d_1^2 \cos^2\theta - N \sin\theta = \rho q (V_1 \cos\theta - V_c) \quad (3)$$

where γ is the specific weight of water, d and V are the water depth and average flow velocity, respectively, N is the reaction from the bed channel on the control volume; here c, f , and l indices refer to critical, pool and downstream sections, respectively.

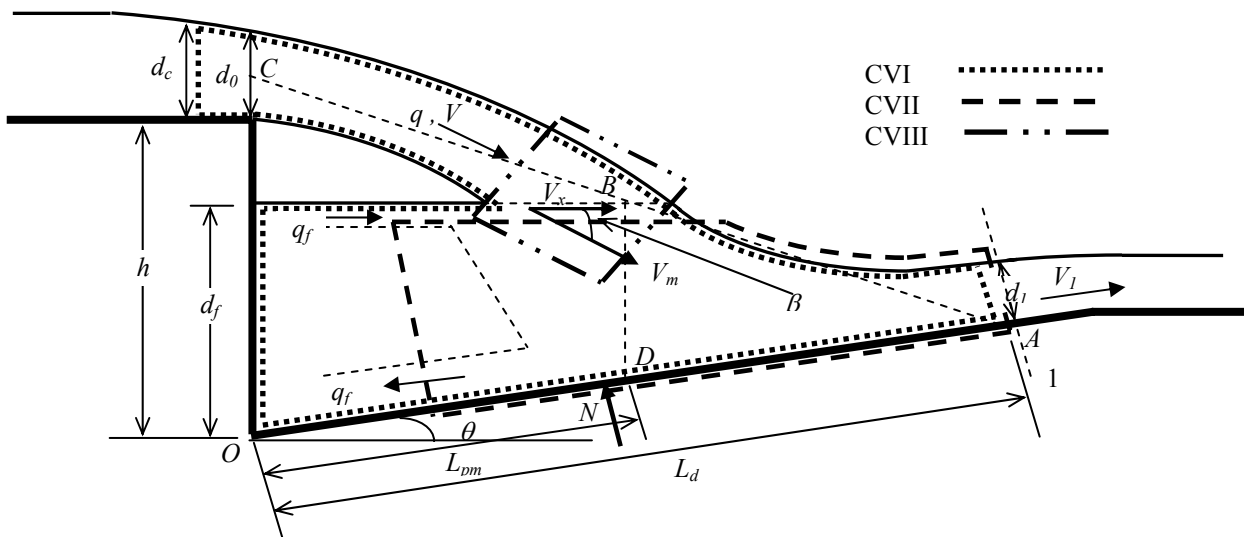


Fig. 4. Schematic sketch for flow over a drop showing the relevant parameters and control volumes

With reference to Fig. 4, it is assumed that three points, A , on the apron at section 1-1, B on the axis of the falling jet at height d_f and , on the axis of the flow at the drop brink, lie on a straight line. This assumption is similar to Rand's assumption [5] for a vertical drop with a horizontal apron. From geometric similarity between OAC and DAB , it is possible to obtain

$$\frac{L_d - L_{pm}}{L_d} = \frac{d_f - L_{pm} \sin \theta}{h + \frac{d_0}{2}} \tag{4}$$

where L is the length from the drop wall, d_0 the brink depth, and indices d and pm refer to downstream section and point D , respectively. If a vertical line is drawn from point B , it intersects the sloping apron at D . If t is the time for the falling jet to travel from point C to point B , the horizontal velocity of the falling jet, V_x , is assumed to be constant from point C to B , and the brink depth is equal to $0.715 d_c$ [5], then from the trajectory equation of the nappe axis,

$$t = \frac{L_{pm} \cos \theta}{V_x} = \frac{0.715 d_c L_{pm} \cos \theta}{q} \quad \text{and} \quad h + \frac{0.715 d_c}{2} - d_f = \frac{1}{2} g t^2 \tag{5}$$

or

$$L_{pm} = \frac{d_c}{\cos \theta} \sqrt{3.912 \frac{h}{d_c} - 3.912 \frac{d_f}{d_c} + 1.398} \tag{6}$$

where $V_x = q/0.715 d_c$. Combining Eqs. (4) and (6), the drop length is given as

$$L_d = \frac{(0.358 d_c + h) \left(\frac{1}{\cos \theta} \right) \sqrt{3.912 \frac{h}{d_c} - 3.912 \frac{d_f}{d_c} + 1.398}}{0.358 + \frac{h}{d_c} - \frac{d_f}{d_c} + \tan \theta \sqrt{3.912 \frac{h}{d_c} - 3.912 \frac{d_f}{d_c} + 1.398}} \tag{7}$$

The next step is to use the impinging jet theory used by White [2] to determine the backward flow in a drop with a horizontal apron. Figure 5 shows a scheme of an impinging jet impacting on a flat surface, which makes the angle β with the jet. In this case, there is nothing to interfere with the flow of water away from the point of impact. It is assumed that the velocity changes only in direction, not in magnitude, and energy loss is negligible. Combining the momentum in the S -direction and continuity principles for the control volume, it can be shown that

$$\frac{W \sin \theta}{\rho V^2 [1 + \cos(\theta + \beta)]} = d_a - \frac{1 - \cos(\theta + \beta)}{1 + \cos(\theta + \beta)} d_b \tag{8}$$

where W is the weight per unit width of the water, and d_a and d_b are the jet thicknesses after the impact point. For $\theta = 0$, Eq. (8) transforms to $d_a/d_b = [1 - \cos(\theta + \beta)]/[1 + \cos(\theta + \beta)]$, obtained by White [2] for a horizontal apron. In the drop case, the lower layer flows into the bottom of the standing pool, causing clockwise rotation, and a return to the jet at exactly the same rate. Assuming that the backward flow is similar to the impinging jet situation, the continuity equation, for CVII results

$$q_f = q \frac{d_a}{d_1} = q \left[\frac{W \sin \theta d_1}{\rho q^2 [1 + \cos(\theta + \beta)]} + \frac{1 - \cos(\theta + \beta)}{1 + \cos(\theta + \beta)} \right] \tag{9}$$

where q_f is the backward circulating unit discharge and d_a is substituted from Eq. (8). It is assumed that the return flow has negligible momentum in the direction of the jet and the total momentum of the jet will not change appreciably in the mixing process [2].

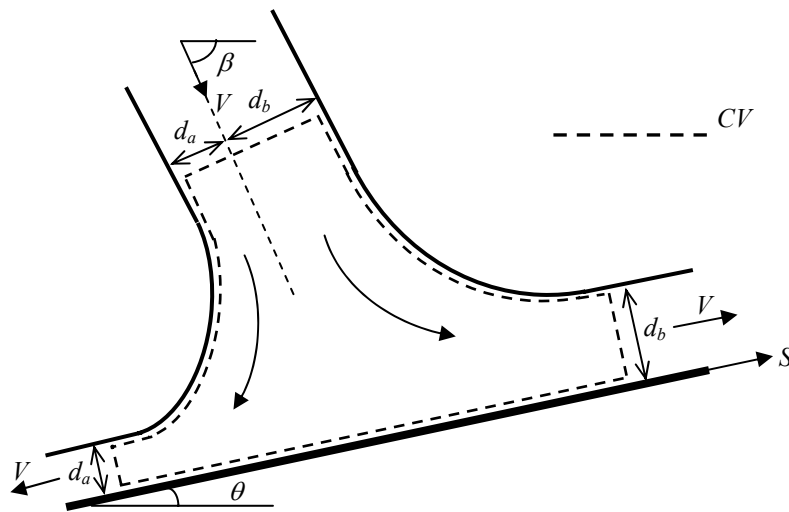


Fig. 5. Schematic sketch for an impinging jet

The momentum equation for the CVIII in Fig. 4 may be written approximately as

$$\rho q V = \rho(q + q_f) V_m \quad (10)$$

where V_m is mean velocity of the thickened flow. Combining Eqs. (9) and (10), the velocity in the thickened zone is shown as

$$V_m = \frac{\rho V q^2 [1 + \cos(\theta + \beta)]}{2\rho q^2 + W d_1 \sin \theta} \quad (11)$$

For $\theta = 0$, Eq. (11) is similar to one used by White [3] and Gill [4].

To determine a relationship between V and the pool depth, d_f , the energy equation for CVI in Fig. 6, assuming negligible energy loss, yields [4]

$$V = \sqrt{2g(h + 1.5d_c - d_f)} \quad (12)$$

Assuming the mean velocity of the thickened flow V_m to remain constant [4], the energy equation for CVII yields (Fig. 6)

$$V_1 = \sqrt{V_m^2 + 2g(d_f - d_1 \cos \theta - L_d \sin \theta)} \quad (13)$$

Combining Eqs. (11), (12), and (13) and considering continuity equation at downstream section as $d_1 = q/V_1$, the following equation yields

$$d_1 = \sqrt{\frac{d_c^3}{2(h + 1.5d_c - d_f) \left\{ \frac{\rho q^2 [1 + \cos(\theta + \beta)]}{2\rho q^2 + W d_1 \sin \theta} \right\}^2 (d_f - d_1 \cos \theta - L_d \sin \theta)}} \quad (14)$$

Gill [4] further argued that the presence of the pool does not appreciably change the horizontal component of the falling jet [5]. This means that the horizontal component of the falling jet velocity before the impact

$$\frac{3}{2} \left(\frac{d_c}{d_1} \right)^2 + \frac{1}{2} \left(\frac{d_f}{d_1} \right)^2 - \frac{1}{2} - \frac{1}{2} \left(\frac{d_f + d_1 + L_d \sin \theta}{d_1^2} \right) L_d \tan \theta - \left(\frac{d_c}{d_1} \right)^3 \left(\frac{1}{\cos \theta} \right) - 1.5 \tan \theta \tan \beta \left(\frac{d_c}{d_1} \right)^2 = 0 \quad (20)$$

Finally, substitute for W from Eq. (19) into Eq. (16)

$$\cos \beta [1 + \cos(\theta + \beta)] = \frac{1.061 \sqrt{d_c} \left[2d_c^3 + L_d d_1 \left(\frac{d_f + d_1 + L_d \sin \theta}{2} \right) \sin \theta \right]}{d_c^3 \sqrt{(h + 1.5d_c - d_f)}} \quad (21)$$

Equations (7), (17), (20), and (21) are used to evaluate flow characteristics at a drop. These four equations are solved simultaneously to determine L_d , d_1 , d_f , and β .

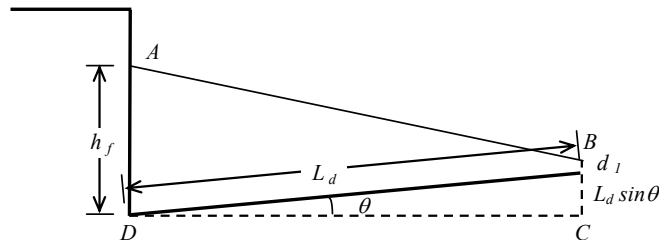


Fig. 7. The designated boundaries for determining the weight

4. ANALYSIS OF EXPERIMENTAL RESULTS

a) Verification of the model for drops with horizontal aprons

If the slope θ of the downstream apron is substituted to zero in the proposed method equations, the characteristics of a drop with a horizontal apron can be determined. Figure 8 shows the variation of the relative pool depth and the relative downstream depth. In Fig. 8, the experimental data and previous model predictions are also presented. Figure 8 shows that predicted values of pool depth agree well with the experimental data and other methods prediction, except for the data of Gill [4] for $h = 4.83$ and 7.40 cm, and White's model predictions [5]. Due to the small height of the drops in Gill's experiment, it is possible that the drops are not ventilated well and negative pressures are produced in the air pocket located between the falling jet and the pool surface. The negative pressure will give rise to a larger pool height. The downstream depth predictions also agree well with the presented data and predictions from other works, except for White's model.

b) Drops with sloping apron

The experimental values of the relative pool and relative downstream depths, and the relative energy loss along with the model predictions are presented Fig. 9. It is found in Fig. 9a that d_f/h' increases due to the increasing of the angle. It is shown that predicted values are somewhat smaller than the experimental results. This is because of the presence of the air in the pool, which increase the height of the pool depth. To find a reasonably general relation for the pool depth, an exponential fit for the pool depth data can be described by the equation

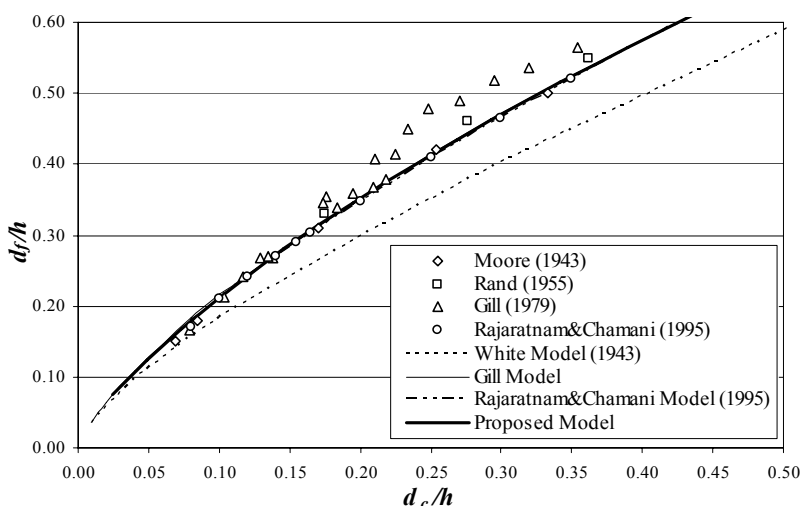
$$\frac{d_f}{h'} = 0.89 \left(\frac{d_c}{h'} \right)^{0.765} \theta^{0.347} \quad (22)$$

with a correlation coefficient $R^2 = 0.992$.

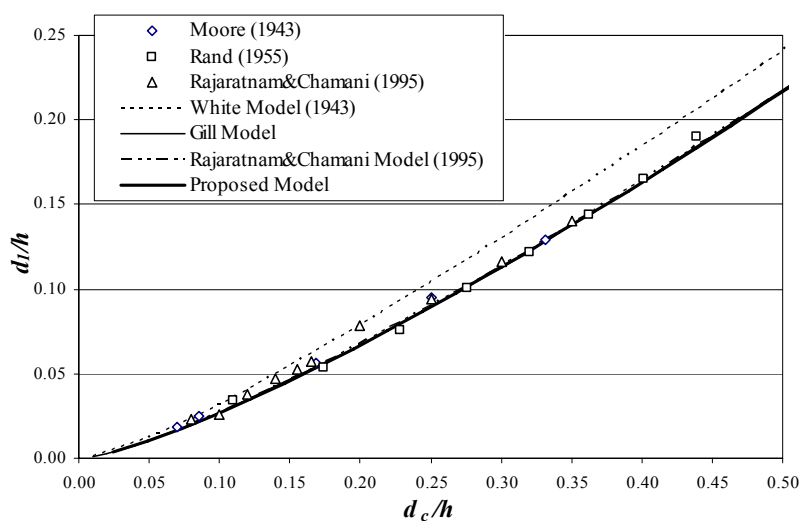
The experimental values of the relative downstream depth along with the data of zero downstream slopes are shown in Fig. 9b. By increasing the discharge for a specific angle, the value of the downstream depth increases. Although the difference between the predictions and the experimental results are insignificant, no systematic evaluation of the effect of the slope on the downstream depth can be seen. The scatter of data is possibly due to the fact that high velocity flow at the base of the drop made the accurate measurement of the flow depth difficult, mainly due to the small water depth and the presence of the air. Most studies reported measurements of a "conservative" or a "mean value" flow depth. These definitions of flow depth, based on the judgment of the observers, influence the accuracy of these measurements and thus the resulting characteristics derived from the flow depth. A best fit for the relative downstream depth data can be described by the equation

$$\frac{d_1}{h'} = 0.516 \left(\frac{d_c}{h'} \right)^{1.184} \theta^{0.045} \tag{23}$$

with a correlation coefficient $R^2 = 0.972$.



(a)



(b)

Fig. 8 Verification of the proposed model for drops with horizontal aprons; (a) Variation of the relative pool depth with d_c/h , (b) Variation of the relative downstream depth with d_c/h

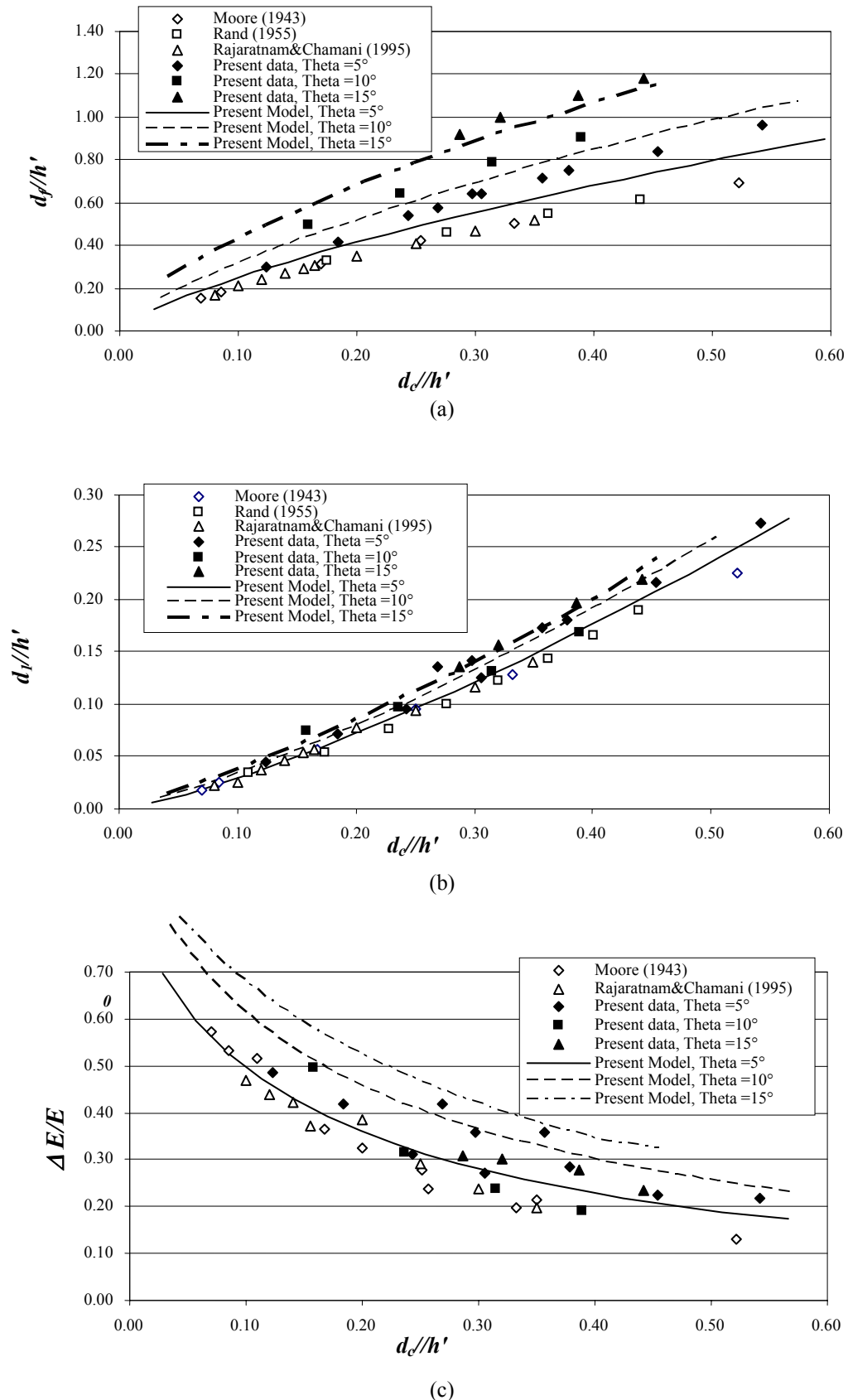


Fig. 9 Characteristics of the drop with sloping apron; a) Variation of the relative pool depth with d_c/h' , b) Variation of the relative downstream depth with d_c/h' , c) Variation of the relative energy loss with d_c/h'

In Fig. 9c, the variation of the relative energy loss with d_c/h' is shown. The relative energy loss is determined as

$$\frac{\Delta E}{E_0} = \frac{E_0 - E_1}{E_0} = 1 - \frac{d_1 \cos \theta + 0.5 d_c^3 / d_1^2 + L_d \sin \theta}{h + 1.5 d_c} \quad (24)$$

where E_0 and E_1 are the upstream and downstream energy, respectively. Again, no definite trend can be seen in the experimental data. As the relative energy loss is proportional to the inverse of d_1^2 , the value of d_1 has a pronounced effect on determining the relative energy loss. As it is mentioned in the previous paragraph, accurate measurement of d_1 is not possible. Thus, the variation of the relative energy loss follows no specific trend. However, for a specific value of d_c/h' , it is found that $\Delta E/E_0$ almost increases with increasing the angle of the sloping invert and the maximum increase is for the 5° degree slope. The variation of the relative energy loss data can be described as

$$\frac{\Delta E}{E_0} = 0.173 \left(\frac{d_c}{h'} \right)^{-0.602} \theta^{-0.079} \quad (25)$$

with a correlation coefficient $R^2 = 0.733$.

5. CONCLUSION

Characteristics of vertical drops with sloping apron at the downstream channel and subcritical flow at the upstream channel have been studied experimentally. Flow characteristics such as pool depth, downstream depth, and energy loss have been measured. Experimental data was compared with the previous investigators' results for horizontal downstream channel. A method is presented to evaluate drop parameters. Two flow regimes have been observed. For small discharges, the flow is subcritical downstream of the drop. By increasing the discharge, the second regime occurs where the flow is supercritical downstream of the drop. In this investigation, the second regime has been studied. It was found that for a specific d_c/h' , the relative pool depth increases with increasing the angle of the sloping inverts. The values of the relative downstream depth for sloping inverts are slightly larger than those with a horizontal downstream channel. Experimental results show that for a specific d_c/h' , the relative energy loss almost increases with increasing the angle of the sloping invert and the maximum increase is for the 5° degree slope. Predictions for the pool and downstream depths agree with the experimental data, but the differences between the predictions and the experimental results of the relative energy loss are significant.

Acknowledgements- The writers would like to thank the Research Council of the Isfahan University of Technology (IUT) and Iran Water Resources Management Organization (IWRMO) for providing financial support.

NOMENCLATURES

d	depth of flow
d_a	backwater impinging jet thickness after the impact point
d_b	forward impinging jet thickness after the impact point
E_0	energy at the upstream of a drop
E_1	energy at the base of a drop
g	gravitational acceleration
h	height of a drop
h'	effective drop height = $h - L_d \sin \theta$
L_d	drop length, the distance along the sloping apron from the drop wall to the position of the depth d_1

L_{pm}	projected distance from the drop wall of the axis of the falling jet at the elevation of d_f along the sloping apron
ℓ	length of the sloping apron
N	bed reaction force
Q	discharge
q	discharge per unit width
q_f	backward circulating unit discharge
V	mean velocity
V_m	mean velocity of the thickened flow
V_x	horizontal mean velocity component of the falling jet
t	time
W	weight of water in the control volume
y_u	tailwater depth above the upstream channel
y_t	tailwater depth above the downstream channel beds
β	falling jet inclination at the pool level
γ	specific weight of water
ΔE	energy loss
λ_a	$\left[\sqrt{g(d_c - y_u)} / (q/y_t) \right]$, dimensionless parameter
λ_b	$\left[\sqrt{g(h' - d_c)} / (q/d_1) \right]$, dimensionless parameter
θ	apron angle with horizontal; and
ρ	density of water

Indices

1	downstream section at the base of the drop
c	critical section; and
f	pool section

REFERENCES

1. Bakhmeteff, B. A. (1932). *Hydraulics of open channels*. McGraw-Hill, p. 295.
2. Moore, W. L. (1943). Energy loss at the base of free overfall. *Transactions, ASCE*, Vol. 108, pp. 1343-1360.
3. White, M. P. (1943). Discussion to energy loss at the base of free overfall. Moore, *Transactions, ASCE*, Vol. 108, pp. 1361-1364.
4. Gill, M. A. (1979). Hydraulics of rectangular vertical drop structures. *J. Hydr. Res.*, Vol. 17, No. 4, pp. 289-302.
5. Rand, W. (1955). Flow geometry at straight drop spillways. *Proceedings, ASCE*, Vol. 81, Paper No. 791, pp. 1-13.
6. Rajaratnam, N. & Chamani, M. R. (1995). Energy loss at drops. *J. Hydr. Res.*, Vol. 33, No. 3, pp. 373-384.
7. Chamani, M. R., Dehghani, A. A. & Beirami, M. K. (2005). Characteristics of drops with sloping invert. *17th Canadian Hydrotechnical Conference*, Edmonton, Canada, August 17-19, pp. 865-870.
8. Wu, S. & Rajaratnam, N. (1996). Submerged flow regimes of rectangular sharp-crested weirs. *J. Hydr. Eng.*, Vol. 122, No. 7, pp. 412-414.
9. Wu, S. & Rajaratnam, N. (1998). Impinging jet and surface flow regimes at drops. *J. Hydr. Res.*, Vol. 36, No. 1, pp. 69-74.